Drought-related changes to geomorphologic processes in central Mali

P. A. JACOBBERGER *Center for Earth and Planetary Studies, National Air and Space Museum, Smithsonian Institution, Washington, D.C. 20560*

ABSTRACT

Geomorphologic evidence exists for repetitive drought conditions in the African Sahel; within this framework of broad climatic changes through time, the 1968–1985 drought episodes are not abnormal. The impact of recent drought on the economies and environments of Sahelian nations has been substantial, however, and the recovery capabilities of severely damaged lands are not well known. Study of the geomorphology and surface processes across a portion of Mali provides some constraints on the responses of desert fringe fluvial systems to changing environmental conditions. Multitemporal orbital image data were used in combination with field investigation to map drought-affected soils, and to document changes to both fluvial and aeolian processes across the region of study. A combination of statistical methods yields consistent evidence of net albedo increases associated with particular landforms and surface processes over a nine-year interval. Although aeolian processes are a significant transport mechanism for removal and redistribution of soil materials, both orbital data and field study indicate that fluvial erosion is responsible for much of the primary topsoil loss and landform modification in this portion of the Sahel.

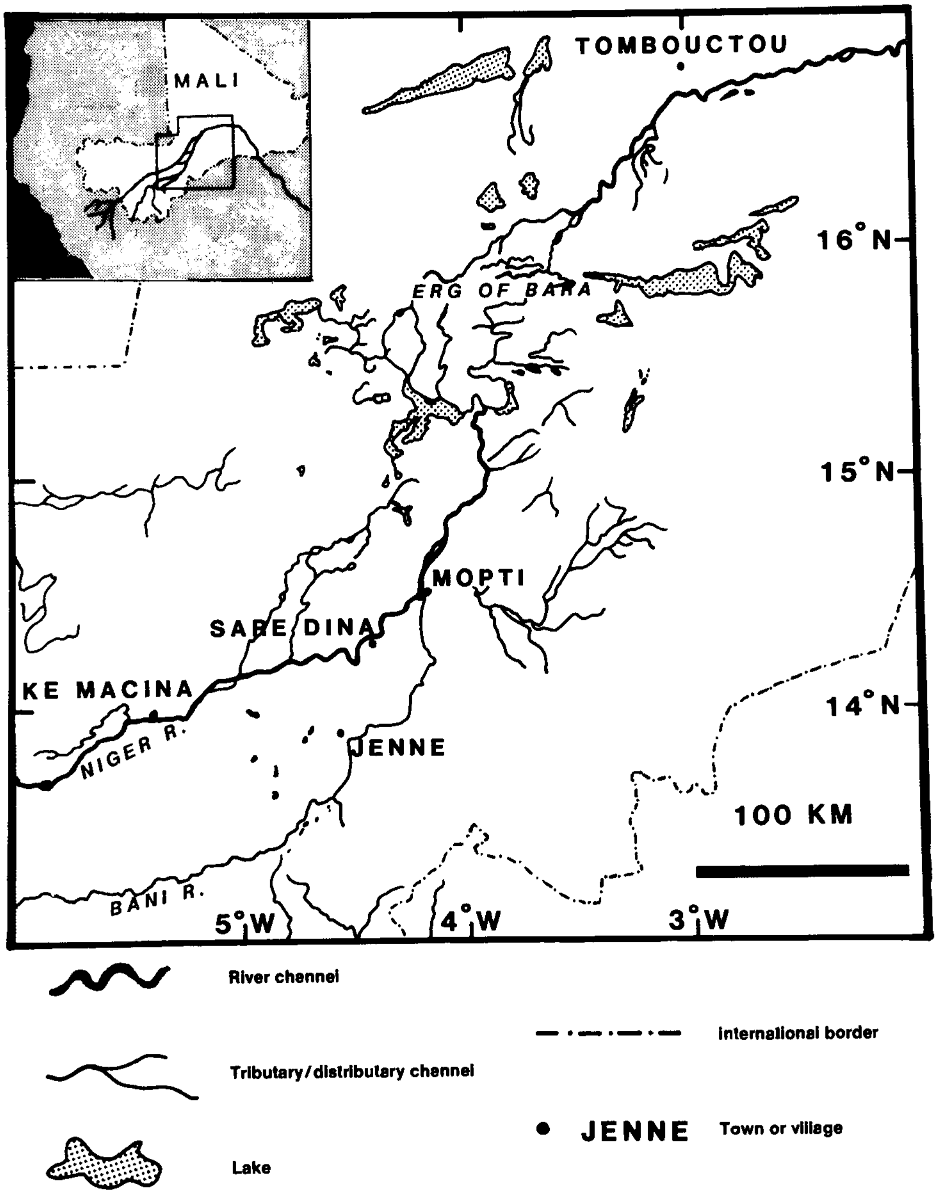

Figure 1. The Inland Niger Delta crosses the Sahel in central Mali and is characterized by the anastomosed system of channels distributary to the Niger River. Mopti marks the confluence of the Niger with a major tributary, the Bani River. Stabilized dunes of the Erg of Bara cross the inland delta north of Mopti; near Tombouctou, the anastomosed reach ends, and the Niger regains a single-channel morphology.

INTRODUCTION

The diversity of landforms in the Sahel attests to the wide variability of Sahelian climate, with conditions ranging from hyperarid to high rainfall over a few thousand years (Grove and Warren, 1968). Stabilized dune cordons exist side-by-side with lacustrine deposits several hundred kilometres south of currently active Saharan dune systems (Talbot, 1980; Street and Grove, 1979; Beaudet and others, 1976). Decadal and interannual rainfall variations are superimposed upon these long-term changes; historical data for Sudano-Sahelian Africa show

Geological Society of America Bulletin, v. 100, p. 351–361, 11 figs., 2 tables, March 1988.

a pattern of abundant rainfall from the 16th through the 18th centuries A.D., interspersed with severe droughts of several years' duration. Drought dominated the early 19th century, with return of higher rainfall late in the century (Nicholson, 1979). Several multi-year droughts occurred in the early 20th century, followed by unusually high rainfall through the 1950s and early 1960s. Recent Sahelian droughts are thus normal, if undesirable, occurrences when considered in the context of the extremely high variability of Sahelian climate.

Drought began in central Mali in 1968 and continued, with brief respites, through 1985. A study of the geomorphologic responses of this area to the recent shifts in precipitation provides some constraints on the long-term consequences of decade-long droughts, and hence some insights into recovery capabilities of affected areas.

The Inland Niger Delta

The Inland Niger Delta is a 400-km-long complex of anastomosing channels distributary to the Niger River in central Mali. The name results from the superficially deltaic morphology of the channel system, which begins near Ké-Macina and flows northeast to Tombouctou (Fig. 1). Annual floods during high-rainfall periods have left thick flood-plain silt deposits throughout the region. The Erg of Bara, a massive cordon of stabilized dunes, crosses the inland delta south of Tombouctou (Tricart, 1959; Talbot, 1980). The 400-km-long complex of channels, dunes, and flood plain received above-average rainfall through the 1950s. Drought began here, as it did elsewhere in the Sahel, in 1968 (UNCOD, 1977), and dry conditions persisted through 1985 and into 1986 (WMO, 1986). Although it has become common to separate the Sahelian drought into two distinct episodes—one in the 1970s and one a continent-wide event in the early 1980s (Brown, 1985)—precipitation records indicate a single event of fluctuating severity from 1968 to present.

A previous study of the geomorphology and hydrology of the upper portion of the Inland Niger Delta incorporated analysis of digital Landsat MSS data taken eight years apart, in 1976 and 1984. These data indicated that localized surface-brightness increases had occurred in the delta between the two scene dates (Jacobberger, 1987). Field mapping in 1985 suggested a relationship between the remotely sensed observations and changes to erosional dynamics and vegetation patterns as a consequence of the prolonged dry conditions, and a correlation between specific landforms and the degree of brightness increase. The objectives of this paper are (1) to document the extent, magnitude, and spatial distribution of brightened surfaces in two study sites (Tombouctou and Mopti) within the inland delta and (2) to relate these to surface conditions and surface processes.

Datasets

Sources of information for this study included remote-sensing data, field mapping and sampling, and monthly precipitation records (summarized in Fig. 2; World Meteorological Organization, 1921–1986). Two Landsat digital multispectral scanner (MSS) scenes were analyzed for each field study site. These scenes were acquired nine years apart, at the height of the dry seasons of 1976 and 1985. Field mapping was conducted at the time of the 1985 acquisitions to provide direct, field-checked, dry-season information, to constrain comparisons with the satellite data acquired nine years earlier (Table 1).

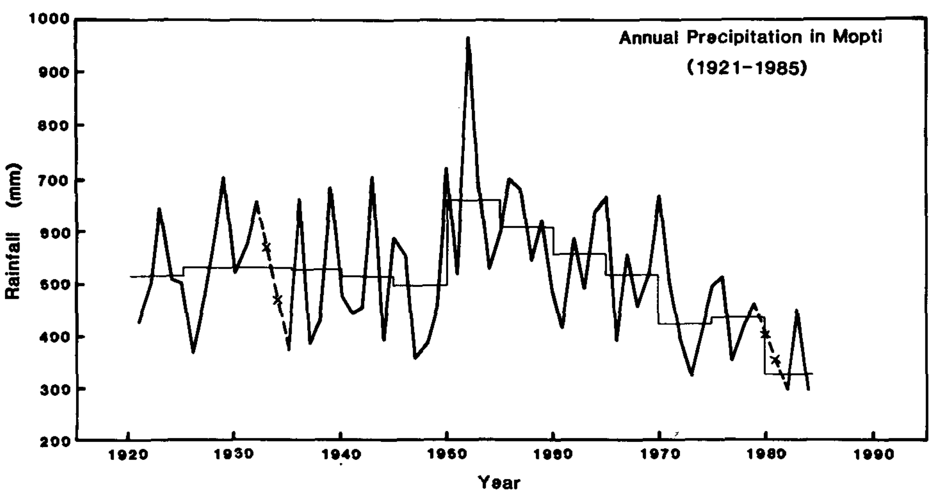

Figure 2. High interannual and decadal rainfall variability are shown by precipitation records for Mopti, 1921–1985. Compared with the high rainfall of the 1950s, both the pre- and post-1950s periods are marked by drought. Heavy line = annual precipitation; fine line = 5-yr averages. "x" signifies incomplete data for that year.

Principal Components Analysis

Principal components analysis has become a common method for investigating the structure of a multivariate dataset (Davis, 1973) and is a highly successful means of extracting information from digital images (Kahle and Rowan, 1980). The basis of principal components analysis is a rigid rotation that orients the coordinate system along directions of major trends within the data (Tatsuoka, 1971). These trends form an ordered series of principal components or vectors containing progressively less amounts of unique information or variance (Anuta, 1977).

If applied to a multichannel image such as a Landsat MSS scene, principal components analysis will clarify the origins of distinct brightness and color trends within the data. The first principal component will define the single brightness and/or color trend that explains the most variance within the data (usually albedo); subsequent components will explain progressively smaller trends related to vegetation, soils, and other sources of variance. If co-registered MSS scenes of different dates are taken together in a principal components analysis, the resulting first component will identify brightness patterns common to all channels of both scenes, that is, areas that have not changed. The second component will identify the important brightness changes between scenes (Byrne and others, 1980). The eigenvector loadings which define these components can be used to relate individual components to sources of variance within the original dataset (Richards, 1984).

Table 2 shows the results of a principal components analysis applied to the combined 1976 and 1985 MSS data for the upper inland delta. The eigenvector loadings explain the relative importance of individual channels to a particular component. The first component shows nearly equal contributions from all channels from both scene dates. The sign reversal across the loadings for the second component indicates that the second largest source of variance within the dataset is the result of brightness changes between scenes. Together, these two components account for more than 96% of the information content within the combined dataset.

TABLE 1. LANDSAT DATA

Scene ID	Acquisition date	Location
2362095035	19 JAN 76	Tombouctou
5035010073	14 FEB 85	Tombouctou
238109564	07 FEB 76	Mopti
5035010082	14 FEB 85	Mopti

In both components, individual spectral channels from each scene contribute nearly equally; the sources of change are related to overall, panchromatic brightness or albedo rather than to strong color trends. In order to simplify subsequent analyses, therefore, the dimensionality of the dataset was reduced by calculating an albedo image from each of the original four-channel datasets (Robinove and others, 1981).

Albedo Calculations

As a measure of overall brightness, the albedo of a surface is a composite indicator of vegetation cover, soil moisture, and other factors related to land condition and use (Otterman, 1974), and therefore albedo changes can be used as indicators of desertification (UNCOD, 1977; Reining, 1978; Courel and Habif, 1983).

Because of the difficulty in determining accurately the atmospheric contribution to brightness within a satellite image, it was not feasible to calculate absolute surface albedos. By examining non-changing control areas in the images, however, the relative atmospheric contribution between two scenes was assessed, and the Landsat data were normalized for atmospheric differences. Albedo changes could then be calculated relative to 1976 levels.

In this study region, few non-changing areas exist, and the best atmospheric control was obtained by using the spectral signatures for 20 villages distributed throughout the field areas. There are several serious assumptions inherent in this approach: (1) that village cores are non-changing areas, (2) that excess brightness due to atmospheric haze is uniform across the scene, and (3) that the change in village brightness due to atmospheric haze is linear and therefore additive. Although this last assumption is commonly made, under Sahelian surface-brightness conditions the assumption may break down. At values of ground reflectance in the range 0.2–0.5, the effects of skylight on space reflectance are minimized; at surface reflectances above 50%, the assumption of linearity will result in an overestimation of the importance of atmospheric haze to scene brightness, with a corresponding underestimation of albedo change (Kondratyev and others, 1974; Otterman and others, 1976, 1980; Richardson, 1982). All villages used for atmospheric corrections were field checked. Villages with significant vegetation were excluded, as were villages smaller than 150 m in diameter (equivalent to four Landsat MSS pixels). Calculations for the remaining villages indicated an atmospheric contribution to brightness of 10% ± 5% for 1985 as compared with 1976.

Following atmospheric normalization, albedos were calculated as a linear combination of the four MSS bands in each scene, and albedo differences (Δa) were obtained by subtraction:

$$\Delta a = \frac{\pi}{I \sin \alpha} \left[\left(\frac{DN_1}{G_1} + \frac{DN_2}{G_2} + \frac{DN_3}{G_3} + \frac{DN_4}{G_4} \right)_{1985} - \left(\frac{DN_1}{G_1} + \frac{DN_2}{G_2} + \frac{DN_3}{G_3} + \frac{DN_4}{G_4} \right)_{1976} \right] \quad (1)$$

where DN_n = digital value in channel n
I = solar irradiance
G_n = gain value for channel n
α = solar elevation angle
(after Robinove and others, 1981).

These differences were plotted as thematic maps of albedo change (see Figs. 3 and 4).

Field Methods

Five weeks were spent in the field, during which a network of foot and vehicle traverses were taken over the study areas. Traverses were irregularly spaced, determined both from early results of satellite analyses and by limitations in access, but with attention to targeting areas of spectral or brightness change as well as morphology. Along traverses, data sheets were used to record surface composition, surface condition and Munsell color, morphologic setting, vegetation type, density and condition, and location on satellite images, at intervals of ~2 km for a total of 413 observations. About 50 representative sediment samples were taken for later analysis. Sediment profiles were examined in distributary channel walls and in pits dug for that purpose. Field locations were photographed.

Subsequent to field work, selected samples were analyzed for size distribution, mineralogy, and (for coarse sediments) grain shape. Results for representative flood-plain deposits are presented in Figure 5.

RESULTS AND DISCUSSION

In both field areas, the spatial distribution and magnitude of brightness increases are correlated with landform units.

TABLE 2. STATISTICS FOR PRINCIPAL COMPONENTS TRANSFORMATION

	1976				1985				
	CH1	CH2	CH3	CH4	CH1	CH2	CH3	CH4	
Means*	23.61	33.59	39.62	33.34	46.55	66.54	71.86	64.99	
S.D.*	8.92	13.92	15.34	12.70	9.84	14.52	15.99	14.48	
C. var.*	0.38	0.41	0.39	0.38	0.21	0.22	0.22	0.22	
EIGENVECTOR MATRIX									% Variance
PC1	0.024	0.025	0.026	0.025	0.026	0.027	0.028	0.027	76.03
PC2	0.027	0.030	0.030	0.029	−0.023	−0.023	−0.023	−0.024	20.33
PC3	0.053	0.040	−0.019	−0.045	0.007	0.009	0.000	−0.013	1.34
PC4	0.044	−0.027	−0.005	0.019	0.064	0.016	−0.017	−0.024	1.06
PC5	−0.073	0.016	0.022	−0.019	0.028	0.024	−0.006	−0.028	0.58
PC6	−0.032	0.030	−0.043	0.043	0.005	0.005	−0.003	−0.004	0.38
PC7	−0.016	0.014	0.002	−0.012	0.058	−0.034	−0.021	0.034	0.20
PC8	0.003	0.000	0.001	−0.002	−0.029	0.037	−0.043	0.028	0.08

Note: Statistics for the transformation are shown for two "stacked" four-channel Landsat MSS images and show the distribution of variance across the dataset. The eigenvector matrix, with each vector presented as a row of individual channel contributions, shows the equal contributions of all channels to PC1, and the high percentage of variance contained in the PC1 vector. PC2 explains more than 20% of the variance inherent in the dataset; the sign reversal across PC2 indicates control of this vector by broad differences between 1976 and 1985 channels of data.

*Means = channel means; S.D. = standard deviation; C. var. = coefficient of variance.

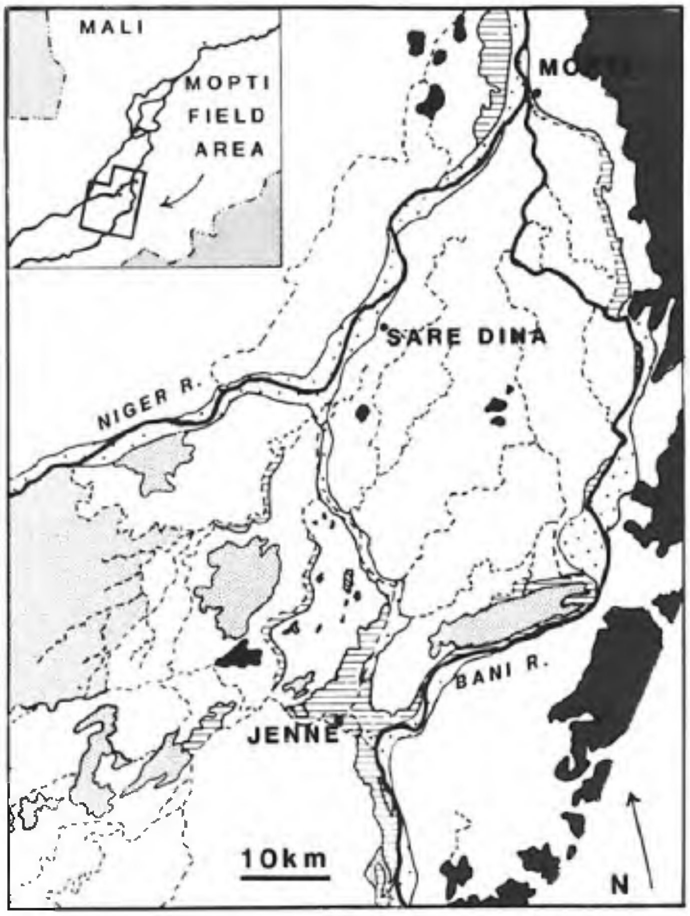

a

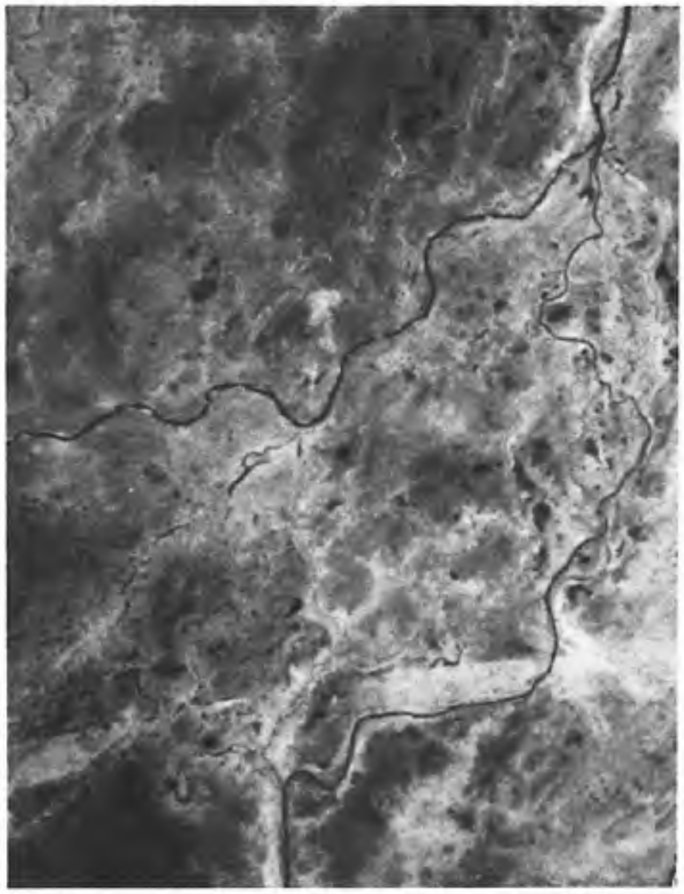

b

Aeolian deposits

Silt and clay levee deposits

Meander scars and scrolls

Floodplain silts

Bandiagara and Koutiala sandstones

Figure 3. The Mopti study site covers a large portion of the upper Inland Niger Delta, a region dominated by anastomosed distributaries of the Niger and Bani Rivers (3a). Albedo images calculated from 1976 and 1985 data are shown in 3b and 3c; the differences between the two scenes are presented in 3d. Areas showing the greatest increases in brightness are dried lakes, followed by levee deposits and aeolian sands.

Mopti

Areas showing greatest albedo increases are those in which water bodies (lakes, ponds, distributary channels) became dessicated over the study interval; these changes average 15% ± 4% in areas where dry soil replaced surface water (Fig. 3). Changes of 7% ± 3% are associated with levees and overbank silt along the Niger and Bani Rivers and their major distributaries in the upper delta. In the field, the surfaces in these areas along watercourses were heavily trampled and pulverized and had no vegetation.

The Niger and Bani Rivers have also increased in brightness (11% ± 6%). In the Niger, sand bars not in evidence in 1976 now line the thalweg. The Bani River in 1985 was less dominated by deposition of coarse material than is the Niger, but was more severely underfit, was shallower (less than 0.5 m west of Jenne), and was highly turbid. In 1984, one year prior to field work, the Bani River had gone dry, and flow in both the Niger and Bani was lower in the early 1980s than had been recorded in the preceding 49 yr (Duncan, 1986). On the Landsat albedo images, total water-surface area in the

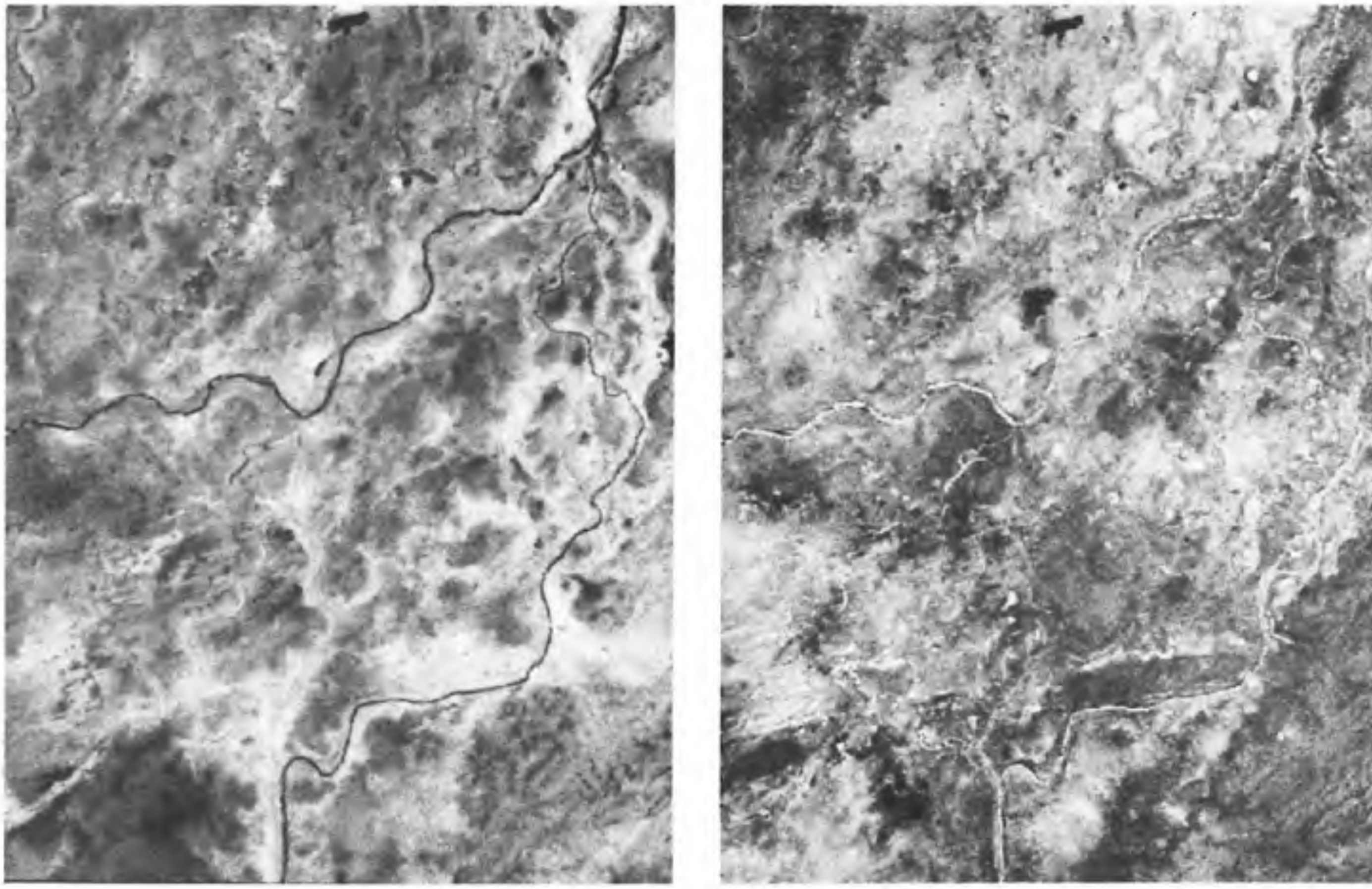

c d

Figure 3. (*Continued*).

upper delta in 1976 was 4% as compared with 1% in 1985.

Flood-plain areas not immediately adjacent to distributaries showed no significant change, and some backswamp areas even showed a slight decrease in brightness (−3% ± 3%). These areas were vegetation covered (ranging from 40% to 70% cover, primarily acacia shrub and bourgou). Surface sediments were consolidated and crusted. Sapping, however, was found in the Niger flood-plain soils, and extensive gullying was observed adjacent to backchannels west of the Bani between Jenne and Mopti (Figs. 6, 7).

Aeolian sand veneers the flood plain west of Jenne, and shows brightness increases of 12% ± 7%. This area was well vegetated in 1976 as determined from the satellite data, but vegetation was sparse in 1985, and wind transport of sand was active.

Village Halos

The existence of a circumscribed, high-albedo "halo" is a characteristic feature of villages and towns in the inland delta; from 1976 to 1985, many of these features have spread and coalesced, as shown around Sare Dina (Fig. 8). These halos are defined in the field by a total lack of vegetation cover, by pulverized soils, and by aeolian transport of the powdery surface silts. Inland delta villages are raised on tells ranging from ~3 to 10 m in height; gullying is ubiquitous at the tell margins (Fig. 9).

Tombouctou

The most striking change in the Tombouctou study site is the increase in brightness of the Niger River flood plain (Fig. 4). Flood-plain margins were from 18% to 39% brighter in 1985, whereas the flood-plain interior was 12% ± 4% brighter. This tremendous increase represents a shift from nearly complete inundation to nearly complete desiccation of the flood plain and concomitant abandonment of distributaries. Surface water covered 25% of the study site in 1976, as compared with just 1% coverage in 1985.

Tombouctou is surrounded by ancient, stabilized sand dunes of the Erg of Azaouad (Talbot, 1980). A distinct bright halo of destabilized sand ~5 km in diameter surrounded Tombouctou in 1976; by 1985, the brightness of the outlying area had increased to the level of the 1976 halo, thus obscuring it (Fig. 10). Field mapping and sampling of the dunes north and east of Tombouctou indicate that this regional brightness increase of 11% ± 3% is due to loss of stabilizing vegetation and resultant surface remobilization

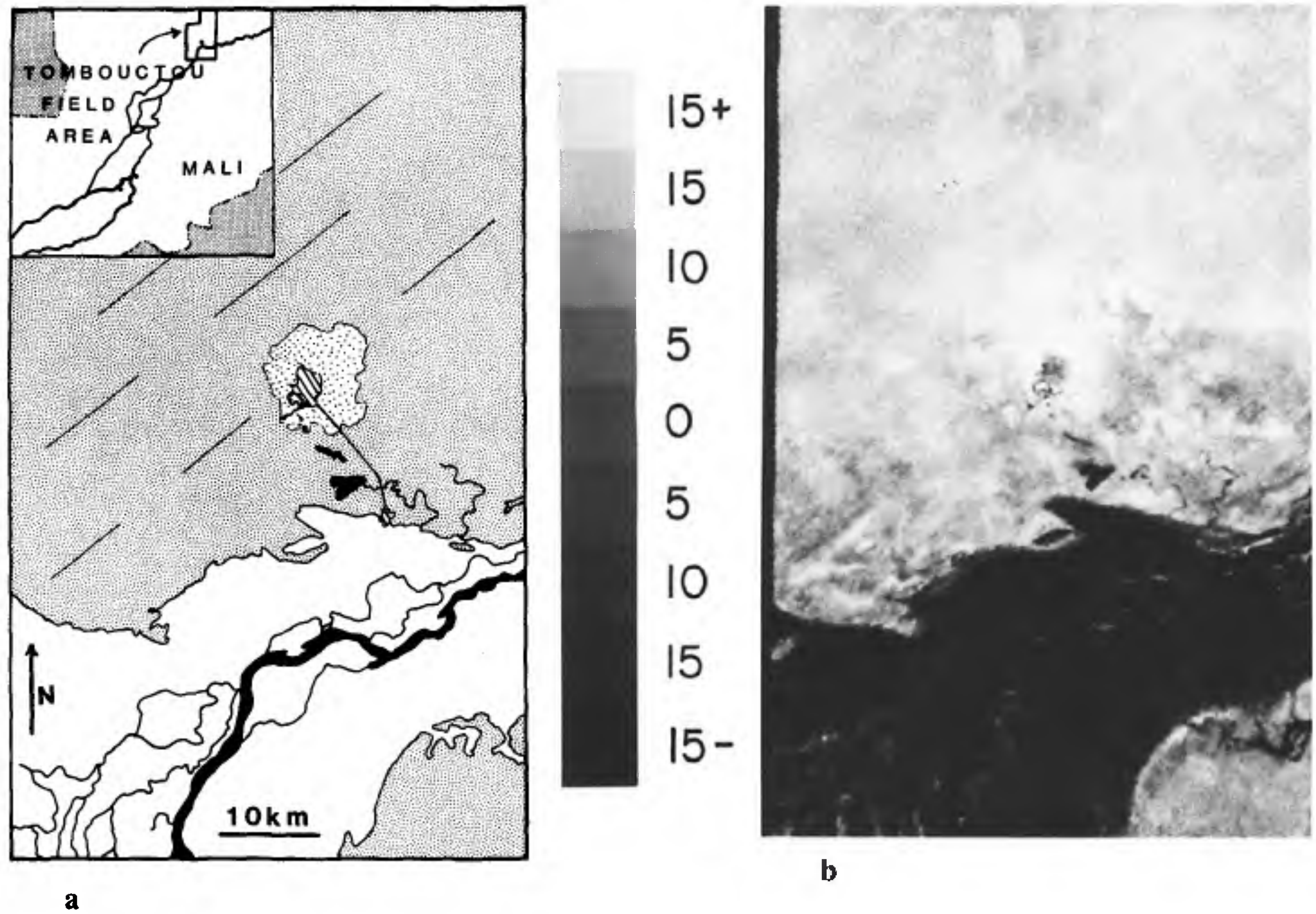

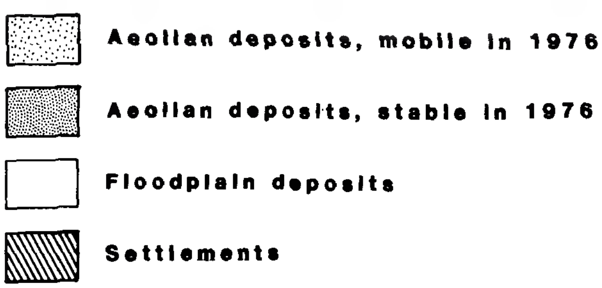

Figure 4. The Tombouctou study site occupies the lower Inland Niger Delta, or Niger bend. South of Tombouctou, the anastomosed reach of the Niger ends, the broad flood plain contracts, and the river regains single-channel morphology; north of the river, Tombouctou is surrounded by stabilized dunes of the Erg of Azaouad (4a). A halo of mobile sand was found to surround the city in 1976. Albedo data for 1976 and 1985 (4b and 4c) show the expansion of this halo and desiccation of the Niger bend flood plain. These changes are summarized in the albedo-difference image of Figure 4d.

of dunes. Trenches dug into dunes 2 km north of Tombouctou reveal stable, reddened, consolidated sand at 30 cm depth.

Implications

The geomorphology of the Inland Niger Delta fits the model-development criteria proposed by Smith and Smith (1980) for the development of anastomosing channel systems: downstream control of base level in an aggradational system (due to blockage by the Erg of Bara) and cohesive banks (sediment predominantly silt sized and originally well vegetated). Overbank areas (dominated by flood ponds and backswamps) are morphologically similar to the anastomosing reaches of rivers in the mountainous alluvial valleys near Banff that Smith and Smith described, despite differences in the climatic and regional settings. The absence of scroll bars and cutoffs across the Niger flood plain, coupled with the steep-walled, narrow, incised morphology of the distributaries, argues for predominantly vertical accretion. Inspection of ex-

Figure 4. (*Continued*).

c

d

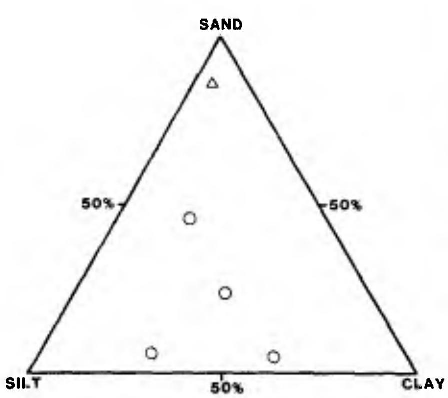

Figure 5. Size distributions for representative flood-plain sediments (open circles). Triangle represents aeolian sand northwest of Jenne.

Figure 6. Sapped soils on the inland delta flood plain.

Figure 7. Gullies developed on overbank sediments northeast of Jenne.

posed strata in distributary walls revealed profiles of uniform silt with neither soil development nor coarse material in the upper 4 m of the sediment column.

The low density of distributary channels in the upper delta recalls the low distributary density of anastomosing reaches along Cooper's Creek, central Australia (Rust, 1981; Nanson and others, 1986). The semi-arid Cooper's Creek system exhibits the low gradient and lack of scroll bars evidenced in the inland delta. Rust (1981) suggested that the discontinuous nature of levees along the channels is likely the reason for the absence of crevassing. Discontinuous levees and a lack of crevassing also characterize the upper inland delta.

Rust suggested that because of the low channel density, accretion proceeds more rapidly in channels than across the flood plain, with the result that distributaries aggrade more quickly than adjacent flood-plain areas, leading to avulsion of blocked channels (Rust, 1981). This may be the case in the upper delta, as shown by the progressive abandonment of aggraded distributaries between the Bani and Niger (Jacobberger, 1987). Levees along the Bani now stand 5–6 m above the 1985 dry-season water level, and both the Bani and associated backpond channels are incising (Jacobberger, 1987). The combination of high levees and reduced flow in the Bani through the drought has restricted flow to the main channel, thus favoring higher erosional energy in the channel and during subsequent overbank flows. Nanson's 1986 model for episodic flood-plain accretion and stripping suggests that vertical accretion can proceed until flood plains effectively become "terraces" above the levee of most flooding, which restricts flow to the main channel resulting in incision. Singular or clustered episodic high-energy floods then scour the flood plain. Until the onset of drought, low-energy flooding of the delta occurred yearly (Touré, 1980), with resulting deposition of fertile silt and organic-rich debris. Although the average annual discharge has been highly variable for both the Niger and Bani, drought-year discharges have declined substantially. In addition, comparisons of 1976 and 1985 well measurements suggest a 2-m decline in static ground-water level during the 9-yr interval (Duncan, 1986).

Although the combination of lowered base level and confined flow should result in incision of the main channels, neither the Niger nor the

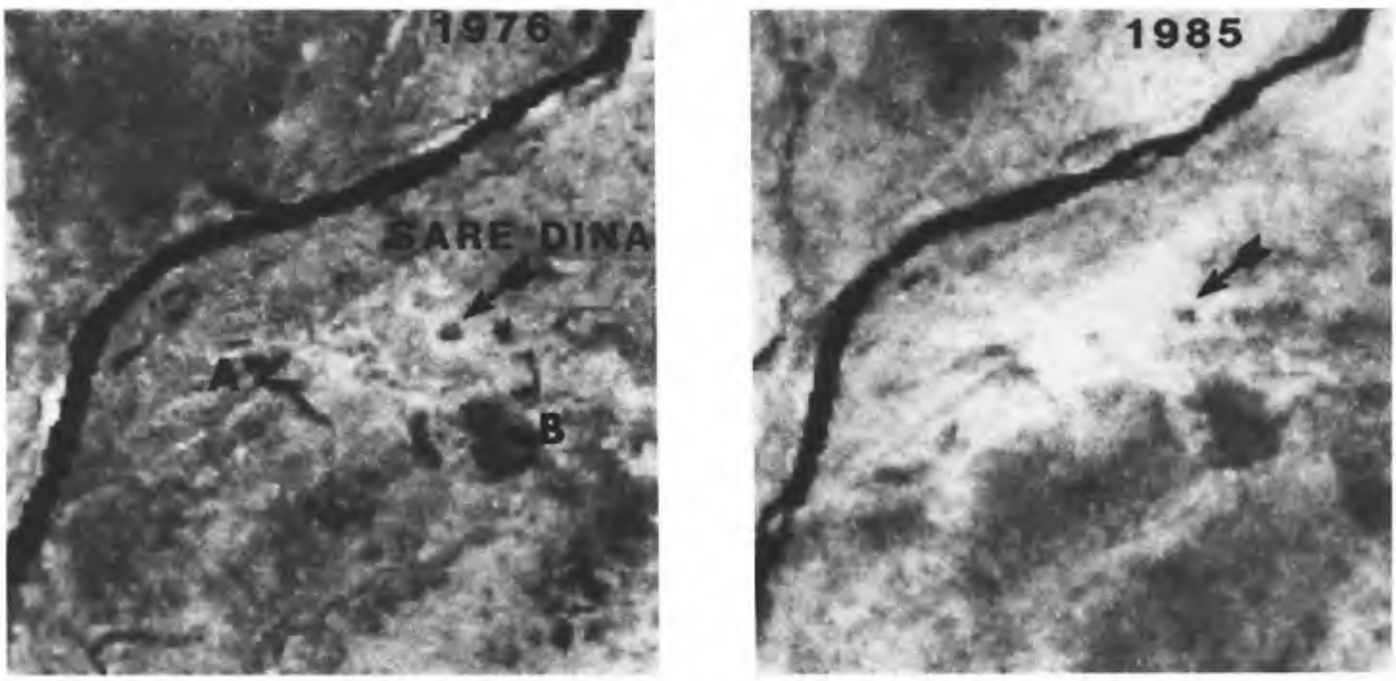

Figure 8. Sare Dina (dark area shown by arrows) is a small village located in the upper delta ~3 km from the Niger River. In 1976, the village was surrounded by a well-defined bright halo. In 1985 image data, the halo has spread to cover adjacent lands. The constriction of the Niger River, the emergence of point bars, and the loss of surface water bodies at (A) and (B) are also visible in 1985 data.

Figure 9. Discontinuous gullies at margins of village tells.

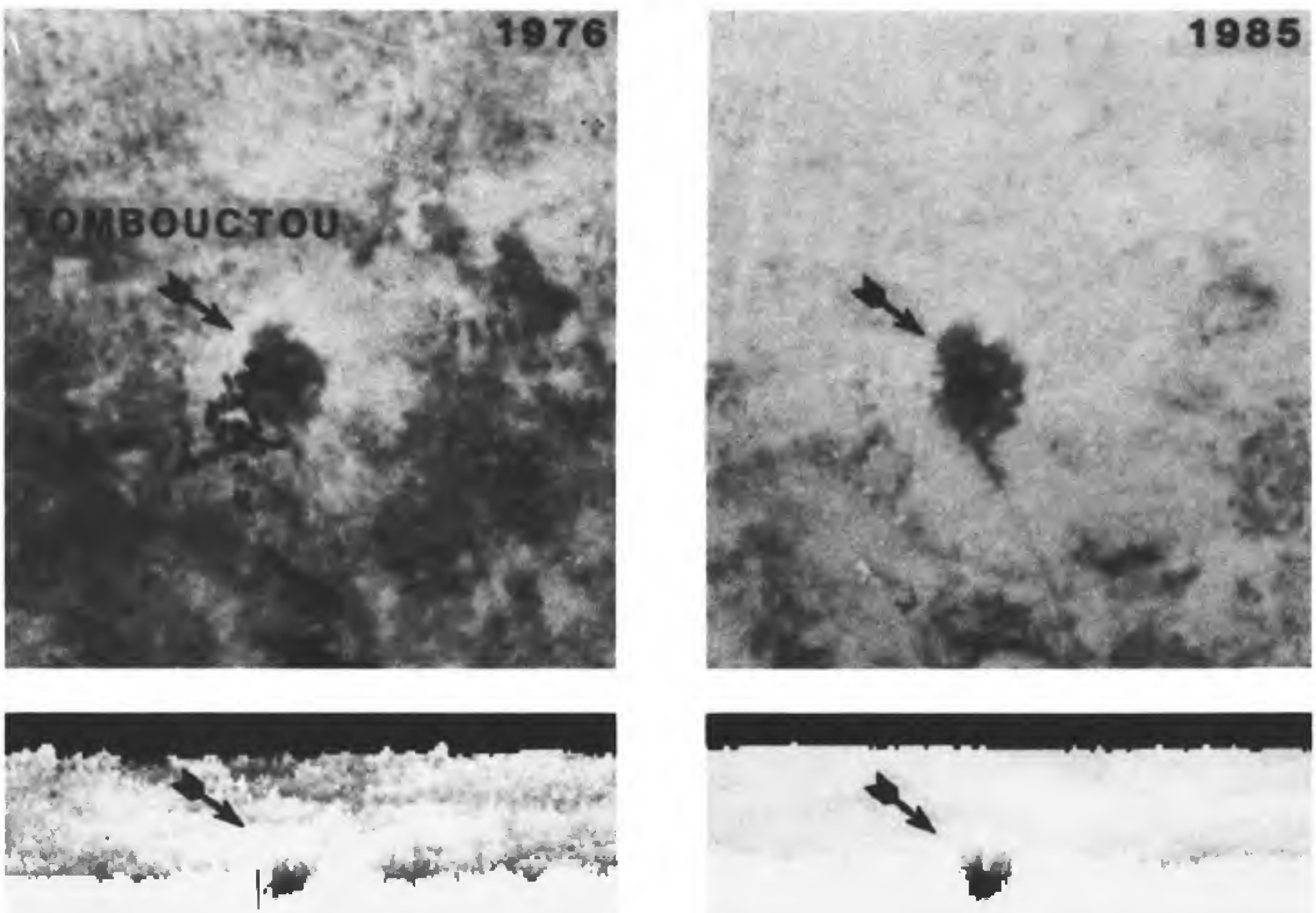

Figure 10. Comparison of 1976 and 1985 albedo images of Tombouctou show expansion of the bright halo of mobile sand around the city, as well as the loss of standing water in the channel that links Tombouctou with the Niger. Albedo profiles presented below the images illustrate the spatial character of these changes. The leading edge of each of these diagrams shows brightness variations along an east-west transect through Tombouctou, and the remainder shows albedo variations north of the city. Coupled with these changes, there is an overall loss of contrast in the 1985 data; this is due partly to real increases in surface brightness and partly to reduced contrast transmissivity as a result of atmospheric dust loading.

Figure 11. Precipitation averages for 5 yr for Mopti are plotted (as arrows) against the Langbein-Schumm curve relating effective precipitation to sediment yield. Although the relationship between effective precipitation and net rainfall is not well constrained for this region, a qualitative trend toward increased sediment yield is indicated (modified after Langbein and Schumm, 1958).

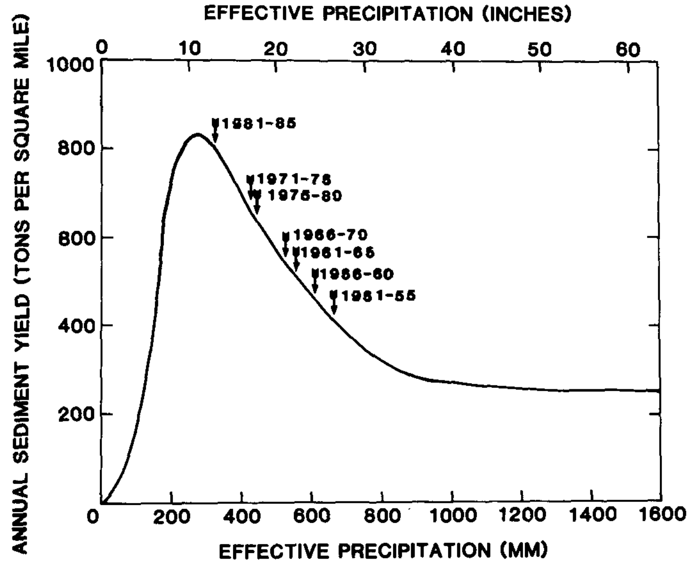

Bani has yet responded with measurable downcutting, although incision of active backchannels of the Bani was observed in the field. The lack of incision of main channels may represent a lapse rate in response of the rivers, or it may be a combined effect of the short observation interval against a low rate of change. On the other hand, main-channel incision may be compensated by the reduced competency of the rivers at the extremely low flow levels of recent years, with ensuing bedload deposition and channel aggradation. Coarse sediments from point bars in the Bani were bimodal, averaging 6 mm and 0.5 mm. Average volumetric flow in the Bani upstream from the inland delta was ~150 m^3/sec in 1983, as compared with 250 m^3/sec in 1976 and a measured high of 900 m^3/sec in 1953 (UNESCO, 1971, 1979; R. C. Duncan, 1986, personal commun.). Low flow rates have also favored abandonment of aggraded distributaries.

Distributary abandonment, together with reduced flood-plain and bank cohesion as a function of reduced vegetation cover, may presage a trend in the Inland Niger Delta system toward a single-channel morphology. A part of the erosional energy resulting from confined flow in main channels will be directed laterally as the river begins to meander successfully due to lowered vegetation density and bank cohesion, as suggested by Smith and Smith (1980). The recent development of point bars and the development of a narrow, discontinuous belt of meander scrolls along the Niger channel suggest the beginning of a meandering tendency, whereas the absence of scrolls and scars across the flood plain suggests that meandering has not been a consistent past process in the Niger system.

The drought-related reduction in natural vegetation cover that factors into the brightness increases observed for the region, coupled with agricultural use of much of the flood plain, argues for increased sediment yield from precipitation-driven fluvial erosion. Langbein and Schumm (1958) demonstrated peak sediment yield at precipitation between 250 and 400 mm/yr. Although their study was restricted to watersheds less than 130 km^2, the form of the curve is essentially controlled by vegetation (Schumm and Harvey, 1982). Measurement uncertainties and the relationship between net rainfall and effective precipitation for this region are poorly constrained; however, qualitative comparison of the Langbein-Schumm curve with rainfall data for Mopti suggests an increase in sediment yield over the course of the drought (Fig. 11).

The cohesive structure, absence of pores or coarse-grained constituents, and lack of organic content of the Niger flood-plain silt provide an impervious surface that favors runoff at the expense of infiltration, perhaps yielding the shallow gullies now developing across the flood plain. In contrast, these same consolidated silt surfaces remained stable under high-wind conditions (as much as 60 km/hr for durations of up to 30 minutes, measured with a hand-held Dwyer windmeter). Silt loosened by mechanical means (trampling, agriculture, or vehicle passage), however, is easily transported. Saltation was observed on dunes and aeolian sand stringers. The association in the upper delta between coarse-grained fluvial deposits and active aeolian features downwind suggests that the local fluvial environment provides the source materials for modern aeolian activity on the flood plain. Near Tombouctou, active aeolian material is predominantly remobilized sand from formerly stable dunes.

CONCLUSIONS

Comparisons of 1976 and 1985 satellite data reveal brightness increases in excess of 15% where lakes, ponds, and distributary streams have dried out. Levee deposits record lesser but consistent increases resulting from erosion and losses of vegetation, moisture, and surface integrity. Similarly, bright areas of damaged soils around villages have expanded over the 9-yr study interval, and brightness increases on vegetated dunes indicate remobilization of formerly stable aeolian landforms. The correlation of satellite-based brightness increases with specific landforms confirms their relationship to surface processes.

Field examination of areas recording change provides insight into the complex response of the Inland Niger Delta through the drought years. Reductions in precipitation and discharge have led to a reduced frequency of overbank deposition. Reductions in flood-plain vegetation density, damage to flood-plain soil integrity, and confined flow in main channels are causing a transition from vertical to lateral accretion and a corresponding increase in the meandering tendency of the main river channels. Concomitant avulsion of distributaries due to aggradation marks a potential abandonment of the anastomosing system as the rivers trend toward single-channel morphology.

In contrast to the multi-channel systems studied by Rust (1981) and Smith and Smith

(1980), definite master streams (the Niger and Bani channels) dominate the anastomosing reach of the Niger system, perhaps speaking for prior episodes of wholesale distributary avulsion during arid climatic episodes. Assuming an end to drought conditions, abandonment of the distributary system would profoundly affect the ability of the river to utilize rainfall. A return to high flow rates confined to the master channel would generate high erosional energy at peak flow; the low permeability of the present surface also favors runoff and erosion, and the result would be catastrophic flooding, flood-plain stripping, and possibly rejuvenation of the distributary system, similar to the sequence predicted by Nanson's (1986) disequilibrium model for flood-plain development.

Assuming continued dry conditions in the inland delta, progressive senescence of the distributary system would have a serious impact on the economy and environment of the region. The delta channel complex acts as a catchment not only for local precipitation, but for water from the highlands in the upper portion of the Niger River basin, 800 km upstream. The delay in flow peak that occurs in the delta is a significant factor in ground-water recharge in central Mali (Touré, 1980). Annual flooding and the presence of the distributary channels form the basis for subsidence agriculture, pastoralism, and transportation in central Mali, and are the major source of soil rejuvenation and recharge for the shallow unconfined aquifers of the region.

The post-drought recovery potential of the Inland Niger Delta (and of other Sahelian regions) depends not only on whether rainfall returns, but on whether the existing hydrologic systems can accommodate rainfall. Aggradation and abandonment of channels, loss of topsoil, and sand encroachment are drought-related processes whose long-term influence on the geomorphologic and hydrologic evolution of the region are far from understood, although the geologic record contains ample evidence for their prior occurrence. In this context, desertification can be thought of as the transition of an environmental system from predominantly fluvial processes to predominantly aeolian activity. Continued study of the response of river systems to extended droughts should shed further light on the evolution, habitability, and recovery potential of desertified lands and desert-fringe regions.

ACKNOWLEDGMENTS

Many thanks are extended to W. G. Nickling, A. L. Bloom, and to an unnamed reviewer for their helpful comments on the manuscript; and to P. L. Strain and F. El-Baz for their suggestions on an early version of the paper. Discussions with R. Duncan, R. J. McIntosh, S. K. McIntosh, and M. Mainguet were most helpful during the analysis phase of the research. H. Traore of the Direction Nationale de la Géologie et des Mines, to S. Diawara and Y. Dabo of the Direction de l'Hydraulique, and to M. Hulbert of the United States Information Agency in Bamako, for their assistance. Sedimentological data were provided by R. Duncan through the courtesy of D. Stanley and H. Sheng, and photographic support was provided by M. Avino and D. Hrabak. Technical assistance was also provided by R. Duncan, D. Hooper, D. Slattery, D. Obler, and R. Aiello. This work was supported by a grant from the Smithsonian Institution Scholarly Studies Program, and by National Aeronautics and Space Administration Contract NAS5-28774.

REFERENCES CITED

Anuta, P. E., 1977, Computer-assisted analysis techniques for remote sensing data interpretation: Geophysics, v. 42, p. 468–481.

Beaudet, G., Michel, P., Nahon, D., Oliva, P., Riser, J., and Ruellman, R., 1976, Formes, formulations superficielles et variations climatiques recentes du Sahara occidental: Revue de Géographie Physique et de Géologie Dynamique, v. 18, p. 157–174.

Brown, L. R., 1985, State of the World report 1985: New York, W. W. Norton and Company, p. 13.

Byrne, G. F., Crapper, P. F., and Mayo, K. K., 1980, Monitoring land-cover change by principal component analysis of multitemporal Landsat data: Remote Sensing of Environment, v. 10, p. 175–184.

Courel, M. F., and Habif, M., 1983, Measurement of changes in Sahelian surface cover using Landsat albedo images: Advances in Space Research, v. 2, p. 37–44.

Davis, J. C., 1973, Statistics and data analysis in geology: New York, John Wiley & Sons, Inc., 550 p.

Duncan, R. C., 1986, Hydrogeologic reconnaissance study, incorporating remotely-sensed data, in a section of Mali, Africa [M.S. thesis]: Moscow, Idaho, University of Idaho, 86 p.

Grove, A. T., and Warren, A., 1968, Quaternary landforms and climate on the south side of the Sahara: Geographical Journal, v. 134, p. 194–208.

Jacobberger, P. A., 1987, Geomorphology of the upper inland Niger delta: Journal of Arid Environments, v. 13, p. 95–112.

Kahle, A., and Rowan, L. C., 1980, Evaluation of multispectral middle infrared aircraft images for lithologic mapping in the East Tintic Mountains, Utah: Geology, v. 8, p. 234–239.

Kamaté, C., 1980, Climat, *in* Traore, M., ed., Atlas du Mali: Paris, les editions jeune afrique, p. 14–17.

Kondratyev, K. Ya., Dyachenko, L. N., and Piatovskaya, N. P., 1974, On the relationship between the Earth-atmosphere system albedo and the Earth's surface albedo, in Earth survey problems: Berlin, Akademie-Verlag, p. 473–482.

McIntosh, R. J., 1983, Floodplain geomorphology and human occupation of the upper inland delta of the Niger: Geographical Journal, v. 149, p. 182–201.

Nanson, G. C., 1986, Episodes of vertical accretion and catastrophic stripping: A model of disequilibrium flood-plain development: Geological Society of America Bulletin, v. 97, p. 1467–1475.

Nanson, G. C., Rust, B. R., and Taylor, G., 1986, Coexistent mud braids and anastomosing channels in an arid-zone river: Cooper Creek, central Australia: Geology, v. 14, p. 175–178.

Nicholson, S. E., 1979, Climatic variations in the Sahel and other African regions during the past five centuries: Journal of Arid Environments, v. 1, p. 3–24.

Otterman, J., 1974, Baring high-albedo soils by overgrazing: A hypothesized desertification mechanism: Science, v. 186, p. 531–533.

——1977, Monitoring surface albedo change with Landsat: Geophysical Research Letters, v. 4, p. 441–444.

Otterman, J., and Fraser, R. S., 1976, Earth-atmosphere system and surface reflectivities in arid regions from Landsat MSS data: Remote Sensing of Environments, v. 5, p. 247–266.

Otterman, J., Ungar, S., Kaufman, Y., and Podolak, M., 1980, Atmospheric effects on radiometric imaging from satellites under low optical thickness conditions: Remote Sensing of Environment, v. 9, p. 115–129.

Palausi, G., 1955, Au sujet du Nigerfossile dans la région de Tombouctou: Revue de Géomorphologie Dynamique, v. 6, p. 217–218.

Reining, P., ed., 1978, Handbook on desertification indicators: Washington, D.C., American Association for the Advancement of Science, 141 p.

Richards, J. A., 1984, Thematic mapping from multispectral image data using the principal components transformation: Remote Sensing of Environment, v. 16, p. 35–46.

Richardson, A. J., 1982, Relating Landsat digital count values to ground reflectance for optically thin atmospheric conditions: Applied Optics, v. 21, p. 1457–1464.

Robinove, C. J., Chavez, P. S., Jr., Gehring, D., and Holmgren, R., 1981, Arid land monitoring using Landsat albedo difference images: Remote Sensing of Environment, v. 11, p. 133–156.

Rust, B. R., 1981, Sedimentation in an arid-zone anastomosing fluvial system: Cooper's Creek, central Australia: Journal of Sedimentary Petrology, v. 51, p. 745–755.

Schumm, S. A., and Harvey, M. D., 1982, Natural erosion in the USA, *in* Kral, D. M., ed., Determinants of soil loss tolerance: American Society of Agronomy Special Publication 45, p. 15–22.

Smith, D. G., and Smith, N. D., 1980, Sedimentation in anastomosed river systems: Examples from alluvial valleys near Banff, Alberta: Journal of Sedimentary Petrology, v. 50, p. 157–164.

Street, F. A., and Grove, A. T., 1976, Environmental and climatic implications of Late Quaternary lake-level fluctuations in Africa: Nature, v. 261, p. 385–390.

——1979, Global maps of lake-level fluctuations since 30,000 yr B.P.: Quaternary Research, v. 112, p. 83–118.

Talbot, M. R., 1980, Environmental responses to climatic change in the West African Sahel over the past 20,000 years, *in* Williams, M.A.J., and Faure, H., eds., The Sahara and the Nile: Rotterdam, A. A. Balkema, p. 37–62.

Tatsuoka, M. M., 1971, Multivariate analysis: Techniques for educational and psychological research: New York, John Wiley & Sons, Inc., 310 p.

Touré, A. I., 1980, Hydrographie, *in* Traore, M., ed., Atlas du Mali: Paris, les editions jeune afrique, p. 12–13.

Tricart, J., 1959, Géomorphologique dynamique de la moyenne vallée du Niger (Soudan): Annales de Géographie, v. 68, p. 333–343.

——1965, Reconnaissance géomorphologique de la Vallée Moyenne du Niger: Dakar, Institut Fondamental d'Afrique Noire, 185 p.

UNCOD (United Nations Conference on Desertification), 1977, Desertification: Its causes and consequences: Oxford, England, Pergamon Press, 448 p.

UNESCO (United Nations Educational, Scientific and Cultural Organization), 1971, Discharge of selected rivers of the world, discharge data from 1922–1964, published by UNESCO, Switzerland, Volume 2, 194 p.

——1974a, Discharge of selected rivers of the world, discharge data from 1965–1969, published by UNESCO, Switzerland, Volume 3, pt. 1, 98 p.

——1974b, Discharge of selected rivers of the world, discharge data from 1969–1972, published by UNESCO, Switzerland, Volume 3, pt. 2, 98 p.

——1979, Discharge of selected rivers of the world, discharge data from 1972–1976, published by UNESCO, France, pt. 3, 104 p.

——1985, Discharge of selected rivers of the World, discharge data from 1976–1979, published by UNESCO, France, pt. 4, 126 p.

World Meteorological Organization, 1921–1986, Monthly climatic data for the world, NOAA/NESDIS National Climatic Data Center, Asheville, North Carolina.

Manuscript Received by the Society September 29, 1986
Revised Manuscript Received June 22, 1987
Manuscript Accepted July 2, 1987